[CANCER RESEARCH 56, 4096–4102, September 15, 1996]

Advances in Brief

Metastatic Prostate Cancer in a Transgenic Mouse[1]

Jeffrey R. Gingrich, Roberto J. Barrios, Ronald A. Morton, Brendan F. Boyce, Francesco J. DeMayo, Milton J. Finegold, Roxani Angelopoulou, Jeffrey M. Rosen, and Norman M. Greenberg[2]

Department of Cell Biology [F. J. D., J. M. R., N. M. G.], Scott Department of Urology [J. R. G., R. A. M., N. M. G.], and Department of Pathology [R. J. B.], Baylor College of Medicine, Houston, Texas 77030; Department of Pathology, Texas Children's Hospital, Houston Texas 77030 [M. J. F.]; Department of Pathology, University of Texas Health Sciences, San Antonio, Texas 78284 [B. F. B.]; and University of Athens Medical School, 11627 Athens, Greece [R. A.]

Abstract

We have previously reported the development of a transgenic mouse model for prostate cancer derived from PB-Tag transgenic line 8247, henceforth designated the TRAMP (transgenic adenocarcinoma mouse prostate) model. We now describe the temporal and spatial consequences of transgene expression and report the identification and characterization of metastatic disease in the TRAMP model. TRAMP mice characteristically express the T antigen oncoprotein by 8 weeks of age and develop distinct pathology in the epithelium of the dorsolateral prostate by 10 weeks of age. Distant site metastases can be detected as early as 12 weeks of age. The common sites of metastases are the periaortic lymph nodes and lungs, with occasional metastases to the kidney, adrenal gland, and bone. By 28 weeks of age, 100% harbor metastatic prostate cancer in the lymph nodes or lungs. We have also demonstrated the loss of normal E-cadherin expression, as observed in human prostate cancer, as primary tumors become less differentiated and metastasize. The TRAMP model provides a consistent source of primary and metastatic tumors for histopathobiological and molecular analysis to further define the earliest molecular events involved in the genesis, progression, and metastasis of prostate cancer.

Introduction

The proportion of patients with clinically and pathologically localized prostate cancer at the time of detection has increased dramatically during the last several years. This has been primarily attributed to an increased public awareness of prostate cancer and prostate cancer screening programs using digital rectal exam, serum testing for prostate-specific antigen, and ultrasound guided transrectal prostatic needle biopsies. Yet despite earlier detection, the number of American men whose deaths will be attributed to prostate cancer continues to increase annually and is estimated to reach more than 41,000 in 1996 (1). Although in younger men with clinically localized prostate cancer and no significant comorbidity the current treatment rationale is for aggressive therapy, a recent report from our institution demonstrated that 23% of patients undergoing radical prostatectomy will still show evidence of disease progression 10 years following surgical intervention (2). If left untreated, prostate cancer will tend to progress at an unpredictably variable but inevitable rate toward an obstructive and metastatic state. To reduce the significant morbidity and mortality, new strategies for the prevention, diagnosis, and treatment of prostate cancer depend on the determination of specific molecular mechanisms involved in the genesis and progression of this disease.

Prostate cancer is essentially unique to humans. The multifocality, heterogeneity, variable clinical progression, propensity to metastasize to bone, and emergence of androgen-independent forms of this disease have exhausted previous attempts to comprehensively study prostate cancer in any single available experimental system. To this end, we have initiated a research program to establish portable inbred transgenic animal models that temporally and spatially develop the progressive stages associated with clinical prostate cancer.

The ability to effectively perturb gene expression in a tissue-specific fashion has generated transgenic mouse models for various human diseases including malignancies of the lymphoid system, skin, mammary gland, liver, and pancreas (for review, see Ref. 3). These studies have demonstrated how well-defined genetic expression systems based on the regulatory elements of genes, viral or cellular in nature, such as the long terminal repeat of the mouse mammary tumor virus, the Eμ immunoglobulin heavy chain enhancer-promoter, and rat insulin promoter, can be exploited to generate transgenic models generally suitable for cancer research.

A prerequisite to establishing a mouse model for prostate cancer was the establishment of a genetic system to target heterologous gene expression specifically to the prostate epithelium. To this end, a minimal regulatory element carrying 426 bp of 5′ flanking sequence and 28 bp of 5′ untranslated sequence of the rat probasin gene (−426/+28 PB) was previously determined to direct expression of the heterologous bacterial *CAT*[3] gene specifically to the secretory epithelial cells of the dorsal, lateral, and ventral lobes of the murine prostate (4). In these studies, expression of the *PB-CAT* transgene was reproducibly observed to be male-specific and developmentally regulated. Consistent with the previous identification and characterization of two distinct androgen response elements within the −426/+28 PB fragment (5), expression of the *PB-CAT* transgene was found to be hormonally regulated in an androgen-specific fashion *in vivo*.

The establishment of the probasin system to target heterologous gene expression specifically to the prostate epithelium facilitated development of an autochtonous inbred transgenic mouse model for prostate cancer (6). In this model, henceforth referred to as the TRAMP model, the PB-SV40 T antigen (*PB-Tag*) transgene was found to be spatially restricted to the dorsolateral and ventral lobes of the prostate and these mice were found to develop progressive forms of prostatic neoplasia. Mild to severe epithelial hyperplasia was observed as early as 10 weeks of age, and invasive adenocarcinoma was observed as early as 18 weeks of age in these mice. *PB-Tag* transgene expression corresponds with sexual maturity, consistent with observations of PB-CAT transgenic mice (4). Since hallmarks of human prostate cancer include the progressive appearance of adenocarcinoma with extracapsular extension, seminal vesicle invasion, and metastasis to lymph nodes, lung, and bone, we have undertaken a careful temporal and spatial histopathological evaluation of the TRAMP model. We now report that these mice develop metastatic prostate cancer and

Received 6/20/96; accepted 7/31/96.

The costs of publication of this article were defrayed in part by the payment of page charges. This article must therefore be hereby marked *advertisement* in accordance with 18 U.S.C. Section 1734 solely to indicate this fact.

[1] This work was supported in part by NIH Prostate Cancer Specialized Program of Research Excellence Grant CA58204 (to N. M. G.) and Grant CA40035 (to B. F. B.), National Cancer Institute Grant CA64851 (to N. M. G.), an award from CaP CURE (to N. M. G.), and American Cancer Society Grant PRTA-21 (to J. R. G.).

[2] To whom requests for reprints should be addressed, at Department of Cell Biology, Baylor College of Medicine, One Baylor Plaza M626, Houston, TX 77030.

[3] The abbreviations used are: CAT, chloramphenicol acetyltransferase; TRAMP, transgenic adenocarcinoma mouse prostate.

Downloaded from http://aacrjournals.org/cancerres/article-pdf/56/18/4096/2461427/cr0560184096.pdf by guest on 24 August 2022

that the pattern of metastatic spread closely reflects that observed in human prostate cancer.

Materials and Methods

Transgenic Animals. Previously described male and female TRAMP mice, heterozygous for the *PB-Tag* transgene, were maintained in a pure C57BL/6 background (Harlan Sprague Dawley, Inc., Indianapolis, IN; Ref. 6). Transgenic males for these studies were routinely obtained as [TRAMP × C57BL/6]F1 or as [TRAMP × FVB]F1 offspring. The isolation of mouse-tail DNA and PCR-based screening assay were performed as described previously (4, 6). All experiments were conducted using the highest standards for humane care in accordance with the NIH Guide for the Care and Use of Laboratory Animals.

Preparation and Analysis of Tissues. Tissues collected at necropsy were routinely fixed in 10% (v/v) phosphate-buffered formalin for 6 h and then transferred to 70% ethanol. Sections (5 μm) were cut from paraffin-embedded tissues and mounted on ProbeOn-Plus slides (Fisher, Houston, TX). Routine sections were stained with H&E. For analysis of bone tissue, including forelimbs, hind limbs, pelvis, ribs, and thoracic and lumbar vertebrae, samples were fixed in 10% (v/v) phosphate-buffered formalin for 48 h, decalcified in 14% EDTA for 14 days, processed through graded alcohols, and embedded in paraffin wax. Sections (4 μm thick) were stained with H&E, orange G, and phloxine.

Immunohistochemical analysis of primary and metastatic sites to detect Tag oncoprotein was performed as described previously (6). Sections were counterstained with eosin. Prostate tissues and metastatic disease sites were subjected to heat-based antigen retrieval (95°C in 10 mM citric acid for 20 min). Immunohistochemical analysis of E-cadherin expression was performed using the HistoMouse kit (Zymed Laboratories, Inc., San Francisco, CA) and a mouse monoclonal antibody to human E-cadherin (Transduction Laboratories, Lexington, KY) with a hematoxylin counterstain. Immunodetection of E-cadherin was graded as normal (uniform cell-cell contact staining) or abnormal (absent or nonspecific staining, not restricted to cell-cell borders; Refs. 7 and 8).

Results and Discussion

Transgene Expression Precedes Prostate Cancer. To correlate the temporal and spatial pattern of transgene expression with the development of prostate cancer in the TRAMP model, histopathological and immunohistochemical analysis was performed on samples obtained at necropsy from 26 transgenic male mice between 8 and 52 weeks of age. Samples of the dorsal, lateral, and ventral lobes of the mouse prostate, as well as the testes, lymph nodes, kidney, spleen, adrenal gland, liver, lung, thymus, brain, and bone, were evaluated and compared to samples procured from nontransgenic littermates. As shown in Fig. 1*A*, a typical dorsolateral prostate from a nontransgenic sexually mature mouse is histologically composed of acini with abundant eosinophilic intralumenal secretions. The acini are lined by a layer of well-organized, columnar secretory epithelium possessing round (basolaterally positioned) nuclei with inconspicuous nucleoli. A single layer of thin, flat, basal epithelial cells with elongated nuclei typically surrounds the columnar epithelium, and a fibromuscular stroma containing 3–4 cell layers of stratified smooth muscle surrounds the acinus. As shown in Fig. 1*B*, the dorsolateral prostate of a TRAMP mouse at 9 weeks of age is entirely similar to that of a nontransgenic mouse except that immunohistochemistry demonstrates abundant nuclear Tag oncoprotein in many epithelial cells. It is interesting to note that these acini still maintain a single regular layer of tall columnar epithelium despite expression of the oncoprotein, demonstrating that transgene expression precedes transformation.

By the time TRAMP mice reach 10–12 weeks of age, dorsolateral prostatic acini display epithelial stratification with some cribriform structures (Fig. 1*C*). In these acini, many epithelial nuclei are elongated and hyperchromatic, with clumping of the chromatin and an increased nuclear to cytoplasmic ratio. Occasional apoptotic bodies and mitotic figures are present at this time. Furthermore, thickening and remodeling of the fibromuscular stroma underlying the abnormal prostatic epithelium are frequently observed. This latter observation is most striking when directly compared to the more normal architecture of an adjacent acinus (Fig. 1*C*). All TRAMP mice examined between 18 and 24 weeks of age (17 of 17) displayed prostatic neoplasia characterized by profound cribriform structures and numerous apoptotic bodies accompanied by marked thickening, remodeling, and hypercellularity of the fibromuscular stroma, as shown in Fig. 1*D*. Although small focal regions of nuclear immunopositive epithelia have occasionally been observed within the anterior prostate gland (data not shown), we have not detected pathology or Tag expression in other tissues.

As demonstrated in this report, TRAMP mice are first observed to develop mild epithelial hyperplasias between 8 and 12 weeks of age, a time corresponding to sexual maturity. It is important to note that expression of Tag has been shown to precede the histological appearance of carcinomas in the TRAMP model, as in other transgenic models (9), suggesting that the proliferative response as a consequence of Tag oncoprotein expression is prerequisite but not sufficient for neoplastic transformation. These observations support the hypothesis that cells expressing the transgene are initially in a preneoplastic state and that other stochastic events are required to confer proliferative advantage and ultimately a malignant state. It is also interesting that transgene expression, as determined by immunohistochemical analysis, is observed to vary both within an individual acinus and between acini within a single gland in the younger mice. Similar observations have been reported in the C3(1)-Tag model (9). However, a uniform pattern of transgene expression is observed in prostate samples procured from mature mice, suggesting that the epithelial cells within a single gland may mature in a fashion that is temporally heterogeneous or that cells expressing the transgene have a growth advantage and replace adjacent cells. It should be interesting to determine whether the mechanisms leading to this temporal heterogeneity contribute to similar temporal heterogeneity observed in human prostate cancer.

Metastatic Prostate Cancer in the TRAMP Model. Metastatic deposits were identified in the lymph node sinuses of 31% (5 of 16) of TRAMP mice between 18 and 24 weeks of age (Fig. 2*A*). To demonstrate that the metastatic cells in the lymph nodes were of prostatic origin, immunohistochemical analysis to detect the T antigen oncoprotein was performed on serial sections. As shown in Fig. 2*B*, immunohistochemistry demonstrates uniform expression of the T antigen oncoprotein confined to the metastatic deposits. The T antigen oncoprotein is clearly not expressed in lymphoid tissue. These observations are in agreement with the tissue-specific pattern of PB-directed transgene expression, as reported previously (4, 6).

Pulmonary metastases were frequently (4 of 11; 36%) identified in the TRAMP mice by 24 weeks of age. These metastases were commonly found in the peribronchiole arteries or in alveolar septae (Fig. 2*C*). Immunohistochemical analysis also demonstrated that the pulmonary metastases expressed the Tag oncoprotein (Fig. 2*D*). Of the TRAMP mice that were over 28 weeks of age, 100% (4 of 4) harbored lymphatic metastases, and 67% (2 of 3) harbored pulmonary metastases. In addition to the metastatic deposits detected in the lymph nodes and lungs, a metastasis displacing the normal upper pole kidney parenchyma has been detected in one mouse at 12 weeks of age (Fig. 2*E*). This metastatic deposit also expressed the T antigen oncoprotein (Fig. 2*F*). Finally, two metastases to the adrenal gland have also been observed (not shown). These observations demonstrate that prostate disease in the TRAMP model predictably progresses from mild to severe hyperplasia, to focal carcinoma, and then to adenocarcinoma that metastasizes beyond the autochtonous site of mice as young as 12

Downloaded from http://aacrjournals.org/cancerres/article-pdf/56/18/4096/2461427/cr0560184096.pdf by guest on 24 August 2022

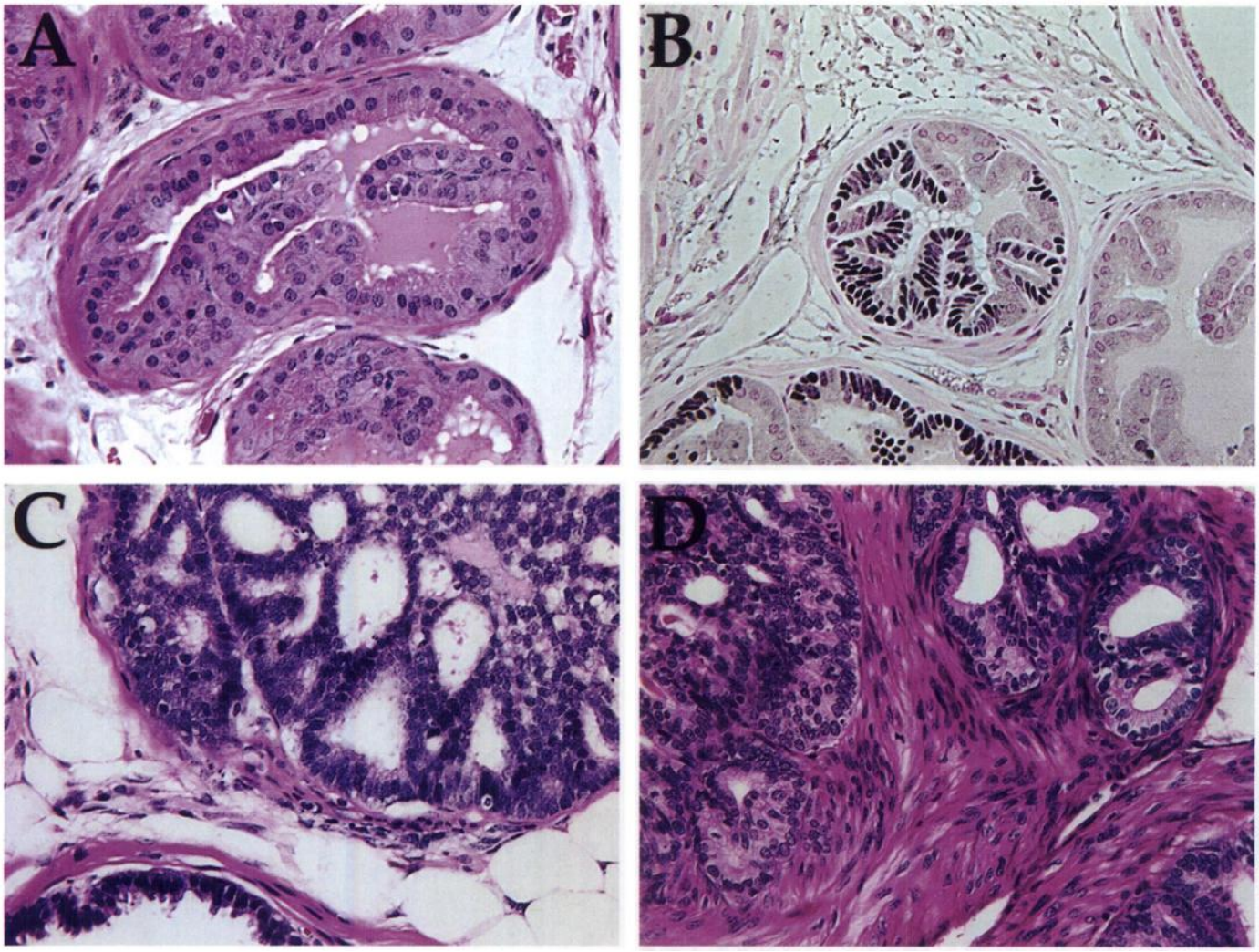

Fig. 1. Histological analysis of prostate cancer in TRAMP mice. *A*, histological section of a dorsolateral prostate from a nontransgenic mouse at 9 weeks of age. The glands are composed of a columnar epithelium with round to oval nuclei. Homogeneous eosinophilic secretion is evident. The stroma is formed by two to three layers of smooth muscle with loose connective tissue found between the glands. H&E; ×40. *B*, immunohistochemical localization of the T antigen oncoprotein in a 9-week TRAMP mouse. Dark regions indicate immunoreactive epithelial nuclear staining in the absence of malignant transformation; 40×. *C*, histological section of a 10-week TRAMP mouse demonstrates epithelial proliferation in a cribriform pattern. Nuclei are hyperchromatic with some apoptotic bodies, and there is minimal stromal hypercellularity. Part of an adjacent normal gland is shown. H&E; 40×. *D*, histological section of a 19-week TRAMP mouse displays major epithelial changes that consist of more solid epithelial neoplastic proliferation although several lumenae are preserved. Marked stromal hypercellularity is noted. H&E; 40×.

weeks of age and that the incidence of metastatic disease progressively increases with time (Fig. 2*G*).

Bone Metastasis and Paraplegia in the TRAMP Model. Interestingly, we have observed hind limb paraplegia in a [TRAMP × FVB]F1 mouse at the age of 22 weeks. Although the primary prostate tumor was not grossly palpable at the time of sacrifice, histological analysis revealed a relatively well differentiated carcinoma with numerous cribriform structures, marked stromal thickening, and hypercellularity (Fig. 3*A*). Immunohistochemical analysis demonstrated uniform epithelial expression of the T antigen oncoprotein in this tumor (Fig. 3*B*). The periaortic lymph nodes of this animal were found to be grossly enlarged and harbored poorly differentiated microscopic metastatic disease in the nodal sinuses (Fig. 3*C*). Again, immunohistochemical analysis demonstrated uniform epithelial expression of the T antigen oncoprotein in the metastatic deposit (Fig. 3*D*). To determine whether the hind limb paraplegia was a consequence of metastatic prostate cancer, a complete skeletal analysis was performed. As shown in Fig. 3*E*, histological examination of decalcified sections of the spine at the level of the thoracolumbar vertebrae revealed that the spinal canal was filled with metastatic tumor. The tumor appeared to have destroyed the spinal cord through pressure atrophy rather than invasion and destruction of the adjacent vertebral bone as typically seen with osteolytic metastatic tumors. Upon closer examination of the interface between the tumor and the bone, an osteoblastic response associated with tumor was detected. At this level, the inner cortical surfaces of the vertebrae were observed to be composed of newly formed woven bone (Fig. 3, *F* and *G*), rather than the lamellar matrix of which this bone and the bone of the posterior spine are typically composed (Fig. 3*G*). As shown in Fig. 3*H*, osteoclasts appear to have resorbed the lamellar matrix adjacent to the tumor cells while osteoblasts were laying down new woven matrix (Fig. 3*G*) in an apparent reparative response. The tumor cells were poorly differentiated and showed no evidence of gland formation. It is also interesting that a similar skeletal analysis of a 34-week-old [TRAMP × C57BL/6]F1 mouse did not reveal any bone pathology (data not shown), suggesting that strain-specific responses as a consequence of transformation may influence frequency of metastasis to distant sites. Additional studies are under way to establish recombinant inbred strains of TRAMP mice to further characterize this potential genetic predisposition to metastatic disease.

Downloaded from http://aacrjournals.org/cancerres/article-pdf/56/18/4096/2461427/cr0560184096.pdf by guest on 24 August 2022

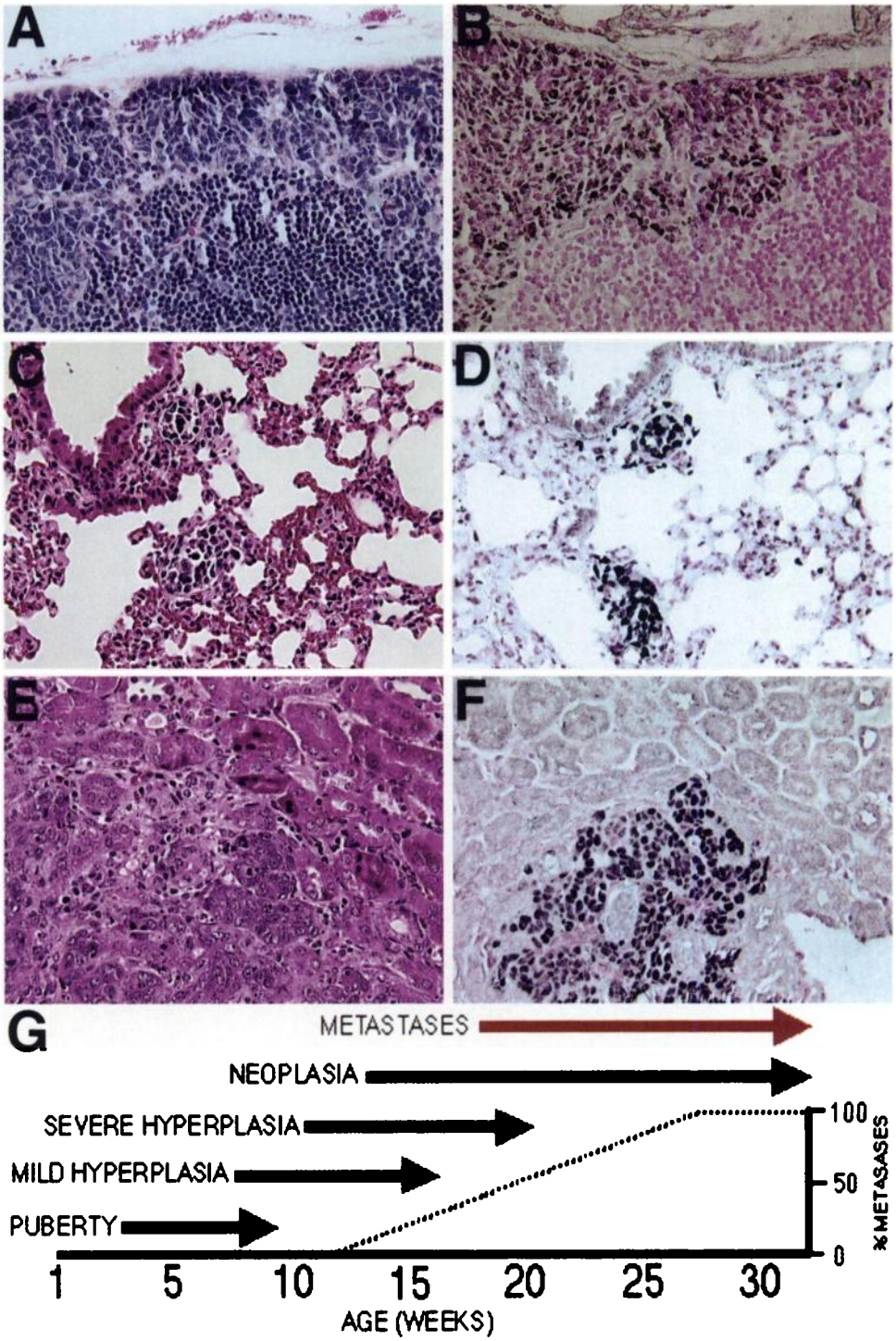

Fig. 2. Histological analysis of metastatic prostate cancer in TRAMP mice. *A*, histological section of a lymph node from a 24-week TRAMP mouse demonstrates partial replacement of the cortex by poorly differentiated epithelial cells. H&E; 40×. *B*, immunohistochemical detection of the T antigen oncoprotein in a step section of *A* demonstrates that the majority of the metastatic cells stain positively; 40×. *C*, histological section of a 24-week TRAMP mouse shows pulmonary parenchyma in which there is blood vessel invasion by malignant cells. H&E; 40×. *D*, immunohistochemical detection of the T antigen oncoprotein in a step section of *C* shows uniform nuclear staining of malignant cells; 40×. *E*, histological section of the kidney in a 12-week TRAMP mouse demonstrates metastatic tumor. H&E; 40×. *F*, immunohistochemical detection of the T antigen oncoprotein in a step section of *E*; 40×. *G*, diagrammatic representation of the temporal development of progressive prostate cancer in the TRAMP model. ·····, incidence of metastatic disease.

The fact that metastasis to the spinal column was observed in a relatively young (23-week-old) mouse with moderately well differentiated primary prostate cancer supports the hypothesis that the molecular mechanisms leading to metastasis can occur quite early in the progression of the disease and that the incidence and frequency of metastasis may not necessarily correlate with primary tumor volume. In fact, a recent study using fluorescent *in situ* hybridization analysis demonstrated that the chromosomal anomalies in metastatic foci in human samples did not necessarily correspond to the chromosomal anomalies contained in the largest or highest grade primary prostate tumor (10). Hence, these observations predict that the chance of any single primary cancer focus acquiring metastatic potential, in either the TRAMP model or human disease, is the stochastic probability that specific mutations will occur to provide survival advantage, a function that is independent of the size or volume of the primary tumor.

E-Cadherin as a Marker of Progression in the TRAMP Model. Various molecular markers of human prostate cancer progression have been reported to have prognostic value. These include the epithelial cell-adhesion molecule E-cadherin (7, 11, 12), Ki-67 (13), and GSTπ (14). Because the loss of functional expression of E-cadherin is consistently associated with the progression of human prostate cancer (7, 8), immunohistochemical analysis was performed

Downloaded from http://aacrjournals.org/cancerres/article-pdf/56/18/4096/2461427/cr0560184096.pdf by guest on 24 August 2022

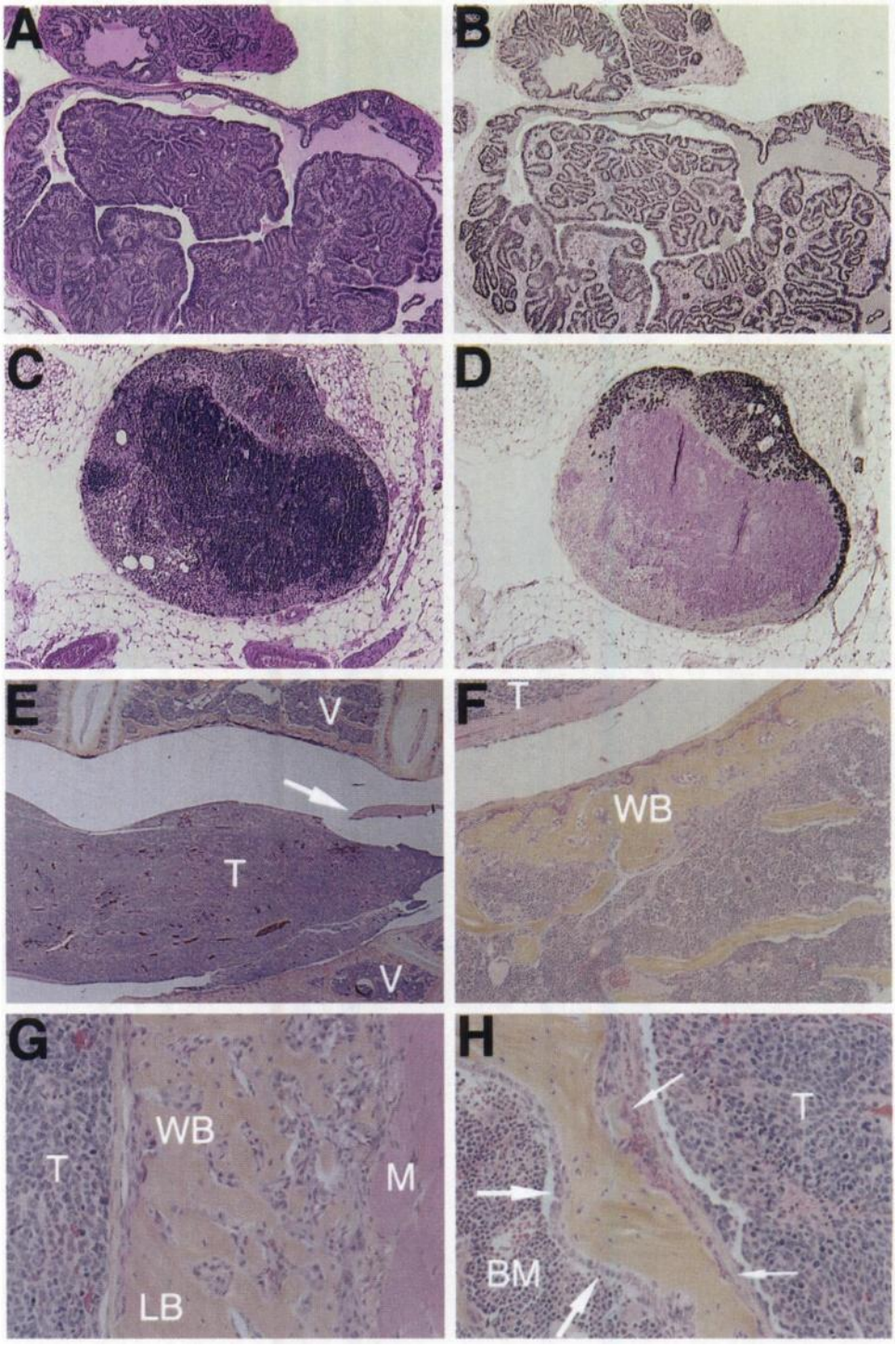

Fig. 3. Histological analysis of metastatic prostate cancer in a paraplegic TRAMP mouse. *A*, histological section of primary prostate tumor shows papillary projections of a well-differentiated tumor lined by columnar epithelium; 10×. *B*, serial histological section of *A* demonstrates immunoreactive oncoprotein in epithelium; 10×. *C*, histological section of lymph node demonstrates a metastatic lesion occupying upper periphery of the node. H&E; 10×. *D*, immunohistochemical analysis of serial section of *C* demonstrates the T antigen oncoprotein; 10×. *E*, a large deposit of metastatic tumor (*T*) is present within the spinal canal at the level of the lower thoracic/lumbar vertebrae (*V*), where it has destroyed most of the spinal cord, only a small fragment of which remains (*arrow*). *F*, higher magnification of the interface between the tumor (*T*) and the adjacent vertebral body shows that the inner surface of the vertebra is composed of irregularly shaped interconnected islands of woven bone (*WB*), rather than a plate of normal lamellar bone. *G*, new woven bone (*WB*) is also being laid down by osteoblasts adjacent to the tumor (*T*) and to preexisting lamellar bone in a posterior spinal process where it abuts striated muscle (*M*). *H*, plump osteoblasts (*large arrows*) are actively laying down bone matrix on the inner cortical surface of a lumbar vertebra adjacent to normal bone marrow (*BM*). Osteoclasts (*small arrows*) are resorbing the bone on the other side of the cortex adjacent to the tumor (*T*), which is composed of sheets of poorly differentiated mononuclear cells with high mitotic and apoptotic rates, but no gland formation.

to characterize the localization of E-cadherin during the development and progression of prostate cancer in the TRAMP model. In these studies, hyperplastic, neoplastic, and metastatic prostate cancer tissue samples procured from TRAMP mice and nontransgenic littermates were analyzed. As shown in Fig. 4*B*, expression of E-cadherin was normally localized to areas of basolateral cell-cell contact in lumenal epithelium of the normal dorsolateral prostate. This is in contrast to the pattern of E-cadherin expression observed in an 18-week-old TRAMP mouse (Fig. 4*C*), where although expression is localized to areas of basolateral cell-cell contact in regions of epithelial hyperplasia and stratification, expression is dramatically reduced in areas with severe hyperplasia and cribriform structures. Furthermore, analysis of metastatic deposits within the lymph nodes demonstrated that E-cadherin expression was very diffuse or absent (Fig. 4*D*). Taken together, these findings demonstrate that a normal pattern of E-cadherin expression is lost during progression of prostate cancer in the TRAMP model in a fashion that parallels observations in human prostate cancer. Because DNA hypermethylation of the E-cadherin 5′ flanking region has been implicated as a molecular mechanism down-regulating E-cadherin expression in human prostate cancer (15), studies are under way to determine whether similar events account for the loss of E-cadherin expression in the TRAMP model (16).

Perspective. Before the development of transgenic models for prostate cancer, the most widely exploited models in prostate cancer

Downloaded from http://aacrjournals.org/cancerres/article-pdf/56/18/4096/2461427/cr0560184096.pdf by guest on 24 August 2022

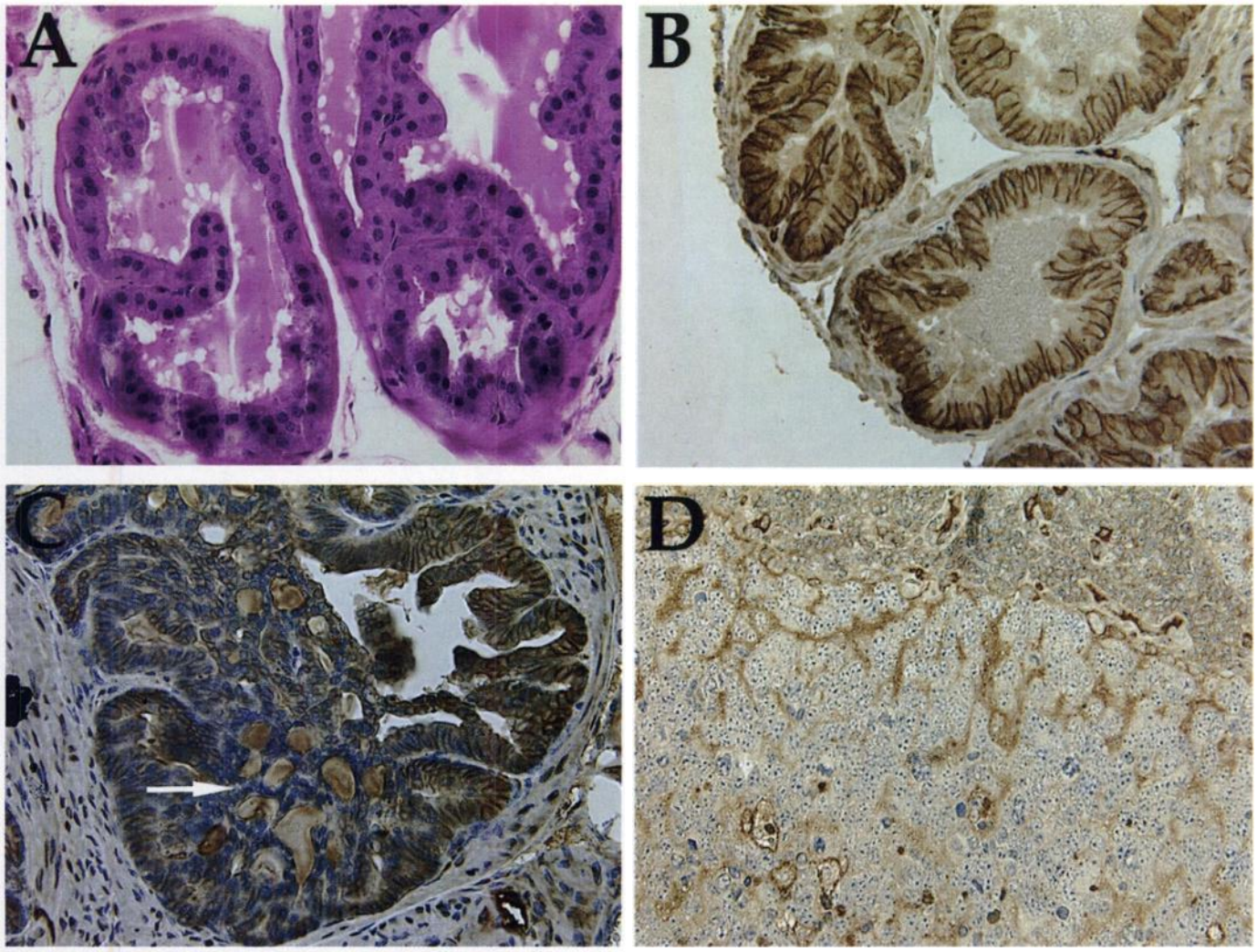

Fig. 4. Immunohistological analysis of E-cadherin expression in metastatic prostate cancer in TRAMP mice. *A*, normal 8-week nontransgenic dorsolateral prostatic acinus. H&E; 40×. *B*, E-cadherin staining at the basolateral cell-cell borders of the epithelia of a 24-week nontransgenic mouse; 40×. *C*, an 18-week TRAMP mouse prostatic acinus displays profound cribriform structures and neoplastic changes. Normal E-cadherin expression is maintained in the relatively normal epithelium basolaterally and on the right portion of the acinus, in contrast to the more hyperplastic areas and cells forming the cribriform structures (*arrow*). *D*, immunohistochemistry of a metastatic lymph node deposit of tumor demonstrates abnormal, poorly localized expression of E-cadherin.

metastasis research were the three human prostate cancer cell lines PC-3, DU-145, and LNCaP. These cells or their derivatives have been shown to metastasize *in vivo* after s.c., i.v., or orthotopic injection in immunodeficient mice (17–19). In addition, the mouse prostate reconstitution model using urogenital sinus cells derived from heterozygous or nullizygous p53 mice has recently been shown to generate prostatic tumors that can metastasize to the lungs, liver, lymph nodes, and bone (20). Whereas each of these model systems has made significant contributions to translational prostate cancer research, transgenic systems, such as TRAMP, in which *PB-Tag* transgene is expressed specifically in the epithelial cells of the murine prostate present a number of distinct advantages over existing models. For example, TRAMP mice develop spontaneous autochtonous disease, whereas human cell lines derived from later metastatic stages of prostate cancer have been subject to potential *in vitro* mutation and selection during passage in tissue culture. Also, TRAMP mice have an intact immune system, whereas human cell lines must be grafted into immunodeficient animals, precluding investigation of the immunobiology related to tumorigenesis and metastasis. Furthermore, TRAMP mice can be used to evaluate therapeutic modalities designed to augment the host immune system surveillance and response to cancer.

Primary pathologies in the TRAMP model that range from mild to severe epithelial hyperplasia with cribriform structures and adenocarcinoma arise with 100% frequency within a 10–24-week period and progress to metastatic stages of prostate cancer, including frequent metastases to the lymph nodes, lung, and occasionally bone. Although each mouse begins with the identical genetic background, stochastic variability in the timing of tumor development and progression can be observed within the population, as is characteristically observed in human prostate cancer. Transgenic systems require very little maintenance other than conventional animal husbandry and can be expanded as needed. Due to their generation in inbred strains of mice, transgenic models can facilitate the establishment of immortalized tissue culture cell lines, which can be studied and manipulated *in vitro* and then reintroduced into syngeneic mice. Finally, primary or metastatic tumors may undergo serial s.c. transplantation studies between syngeneic hosts, providing an expanded source of similar tumor samples. Both cell lines and a transplantable tumor model are currently being characterized in our laboratory.[4]

[4] B. Foster and J. Gingrich, manuscripts in preparation.

Downloaded from http://aacrjournals.org/cancerres/article-pdf/56/18/4096/2461427/cr0560184096.pdf by guest on 24 August 2022

The TRAMP model will provide the research community with a replenishable source of primary and metastatic tumors for histopathobiological and molecular analysis. It is anticipated that such studies will further define the molecular mechanisms underlying the initiation, development, and progression of prostate cancer. Lastly, TRAMP mice provide a suitable animal model to identify and test promising new chemopreventive and therapeutic strategies for the prevention and treatment of human prostate cancer.

Acknowledgments

We thank Hyun Nahm for expert technical assistance and preparation of the histological sections, Angela Major and Lisa Madewell for immunohistochemical analysis, Shu-Wen Sun and Louise Hadsell for transgenic animal husbandry, and Kelly Bevans for administrative support.

References

1. Parker, S. L., Tong, T., Bolden, S., and Wingo, P. A. Cancer statistics 1996. CA Cancer J. Clin., *46:* 5–27, 1996.
2. Ohori, M., Wheeler, T. M., Kattan, M. W., Goto, Y., and Scardino, P. T. Prognostic significance of positive surgical margins in radical prostatectomy specimens. J. Urol., *154:* 1818–1824, 1995.
3. Adams, J. M., and Cory, S. Transgenic models of tumor development. Science (Washington DC), *254:* 1161–1167, 1991.
4. Greenberg, N. M., DeMayo, F. J., Sheppard, P. C., Barrios, R., Lebovitz, R., Finegold, M., Angelopoulou, R., Dodd, J. G., Duckworth, M. L., Rosen, J. M., and Matusik, R. J. The rat probasin gene promoter directs hormonally- and developmentally-regulated expression of a heterologous gene specifically to the prostate in transgenic mice. Mol. Endocrinol., *8:* 230–239, 1994.
5. Rennie, P. S., Bruchovsky, N., Leco, K. J., Sheppard, P. C., McQueen, S. A., Cheng, H., Snoek, R., Hamel, A., Bock, M. E., MacDonald, B. S., Nickel, B. E., Chang, C., Liao, S., Cattini, P. A., and Matusik, R. J. Characterization of two cis-acting DNA elements involved in the androgen regulation of the probasin gene. Mol. Endocrinol., *7:* 23–36, 1993.
6. Greenberg, N. M., DeMayo, F., Finegold, M. J., Medina, D., Tilley, W. D., Aspinall, J. O., Cunha, G. R., Donjacour, A. A., Matusik, R. J., and Rosen, J. M. Prostate cancer in a transgenic mouse. Proc. Natl. Acad. Sci. USA, *92:* 3439–3443, 1995.
7. Umbas, R., Schalken, J. A., Aalders, T. W., Carter, B. S., Karthaus, H. F., Schaafsma, H. E., Debruyne, F. M., and Isaacs, W. B. Expression of the cellular adhesion molecule E-cadherin is reduced or absent in high-grade prostate cancer. Cancer Res., *52:* 5104–5109, 1992.
8. Umbas, R., Isaacs, W. B., Bringuier, P. P., Schaafsma, H. E., Karthaus, H. F., Oosterhof, G. O., Debruyne, F. M., and Schalken, J. A. Decreased E-cadherin expression is associated with poor prognosis in patients with prostate cancer. Cancer Res., *54:* 3929–3933, 1994.
9. Maroulakou, I. G., Anver, M., Garrett, L., and Green, J. E. Prostate and mammary adenocarcinoma in transgenic mice carrying a rat C3(1) simian virus 40 large tumor antigen fusion gene. Proc. Natl. Acad. Sci. USA, *91:* 11236–11240, 1994.
10. Qian, J. Q., Bostwick, D. G., Takahashi, S., Borell, T. J., Herath, J. F., Lieber, M. M., and Jenkins, R. B. Chromosomal anomalies in prostatic intraepithelial neoplasia and carcinoma detected by fluorescence *in situ* hybridization. Cancer Res., *55:* 5408–5414, 1995.
11. Bussemakers, M. J., van Moorselaar, R. J., Giroldi, L. A., Ichikawa, T., Isaacs, J. T., Takeichi, M., Debruyne, F. M., and Schalken, J. A. Decreased expression of E-cadherin in the progression of rat prostatic cancer. Cancer Res., *52:* 2916–2922, 1992.
12. Mareel, M. M., Behrens, J., Birchmeier, W., De Bruyne, G. K., Vleminckx, K., Hoogewijs, A., Fiers, W. C., and Van Roy, F. M. Down-regulation of E-cadherin expression in Madin Darby canine kidney (MDCK) cells inside tumors of nude mice. Int. J. Cancer, *47:* 922–928, 1991.
13. Bubendorf, L., Sauter, G., Moch, H., Schmid, H. P., Gasser, T. C., Jordan, P., and Mihatsch, M. J. KI67 labelling index: an independent predictor of progression in prostate cancer treated by prostatectomy. J. Pathol., *178:* 437–441, 1996.
14. Lee, W. H., Morton, R. A., Epstein, J. I., Brooks, J. D., Campbell, P. A., Bova, G. S., Hsieh, W. S., Isaacs, W. B., and Nelson, W. G. Cytidine methylation of regulatory sequences near the pi-class glutathione *S*-transferase gene accompanies human prostatic carcinogenesis. Proc. Natl. Acad. Sci. USA, *91:* 11733–11737, 1994.
15. Graff, J. R., Herman, J. G., Lapidus, R. G., Chopra, H., Xu, R., Jarrard, D. F., Isaacs, W. B., Pitha, P. M., Davidson, N. E., and Baylin, S. B. E-cadherin expression is silenced by DNA hypermethylation in human breast and prostate carcinomas. Cancer Res., *55:* 5195–5199, 1995.
16. Morton, R. A., Gingrich, J. R., Foster, B. A., Madewell, L., and Greenberg, N. M. E-cadherin expression in a transgenic animal model of metastatic prostate cancer. J. Urol., *155:* 514A, 1996.
17. Lee, C., Shevrin, D. H., and Kozlowski, J. M. *In vivo* and *in vitro* approaches to study metastasis in human prostatic cancer. Cancer Metastasis Rev., *12:* 21–28, 1993.
18. Stephenson, R. A., Dinney, C. P., Gohji, K., Ordonez, N. G., Killion, J. J., and Fidler, I. J. Metastatic model for human prostate cancer using orthotopic implantation in nude mice. J. Natl. Cancer Inst., *84:* 951–957, 1992.
19. Thalmann, G. N., Anezinis, P. E., Chang, S. M., Zhau, H. E., Kim, E. E., Hopwood, V. L., Pathak, S., von Eschenbach, A. C., and Chung, L. W. Androgen-independent cancer progression and bone metastasis in the LNCaP model of human prostate cancer. Cancer Res., *54:* 2577–2581, 1994.
20. Thompson, T. C., Park, S. H., Timme, T. L., Ren, C., Eastham, J. A., Donehower, L. A., Bradley, A., Kadmon, D., and Yang, G. Loss of p53 function leads to metastasis in ras+myc-initiated mouse prostate cancer. Oncogene, *10:* 869–879, 1995.

Downloaded from http://aacrjournals.org/cancerres/article-pdf/56/18/4096/2461427/cr0560184096.pdf by guest on 24 August 2022